Photodissociation dynamics of fluorobenzene (C 6 H 5 F) at 157 and 193 nm : Branching ratios and distributions of kinetic energy

Shih-Huang Lee, Chia-Yan Wu, Sheng-Kai Yang, and Yuan-Pern Lee

Citation: The Journal of Chemical Physics **125**, 144301 (2006); doi: 10.1063/1.2353118
View online: http://dx.doi.org/10.1063/1.2353118
View Table of Contents: http://scitation.aip.org/content/aip/journal/jcp/125/14?ver=pdfcov
Published by the AIP Publishing

Photodissociation dynamics of fluorobenzene (C_6H_5F) at 157 and 193 nm: Branching ratios and distributions of kinetic energy

Shih-Huang Lee[a),b)]
National Synchrotron Radiation Research Center (NSRRC), 101 Hsin-Ann Road, Hsinchu Science Park, Hsinchu 30076, Taiwan

Chia-Yan Wu and Sheng-Kai Yang
Department of Chemistry, National Tsing Hua University, Hsinchu 30013, Taiwan

Yuan-Pern Lee[a),c)]
Department of Applied Chemistry and Institute of Molecular Science, National Chiao Tung University, Hsinchu 30010, Taiwan; and Institute of Atomic and Molecular Sciences, Academia Sinica, Taipei 10617, Taiwan

(Received 21 July 2006; accepted 16 August 2006; published online 9 October 2006)

Following photodissociation of fluorobenzene (C_6H_5F) at 193 and 157 nm, we detected the products with fragmentation-translational spectroscopy by utilizing a tunable vacuum ultraviolet beam from a synchrotron for ionization. Between two primary dissociation channels observed upon irradiation at 193 (157) nm, the HF-elimination channel $C_6H_5F \rightarrow HF+C_6H_4$ dominates, with a branching ratio of 0.94 ± 0.02 (0.61 ± 0.05) and an average release of kinetic energy of 103 (108) kJ mol^{-1}; the H-elimination channel $C_6H_5F \rightarrow H+C_6H_4F$ has a branching ratio of 0.06 ± 0.02 (0.39 ± 0.05) and an average release of kinetic energy of 18.6 (26.8) kJ mol^{-1}. Photofragments H, HF, C_6H_4, and C_6H_4F produced via the one-photon process have nearly isotropic angular distributions. Both the HF-elimination and the H-elimination channels likely proceed via the ground-state electronic surface following internal conversion of C_6H_5F; these channels exhibit small fractions of kinetic energy release from the available energy, indicating that the molecular fragments are highly internally excited. We also determined the ionization energy of C_6H_4F to be 8.6 ± 0.2 eV.
 [DOI: 10.1063/1.2353118]

I. INTRODUCTION

Numerous channels are energetically accessible upon photodissociation of benzene at 193 nm.[1] The major channel is H elimination,[2–4] whereas channels $C_6H_4+H_2$ and $C_5H_3+CH_3$ are minor; these two channels are controversially attributed either to a one-photon process[2] or to a two-photon process.[4] Substituted benzenes show different behaviors in photodissociation. Upon irradiation at 193 nm, toluene undergoes fragmentation via two major channels to yield $H+C_6H_5CH_2$ and $CH_3+C_6H_5$; it isomerizes to a seven-membered ring followed by aromatization before fragmentation.[5] Photodissociation of a phenyl halide is less complicated than that of benzene and toluene. Reports on photodissociation of C_6H_5Cl,[6–10] C_6H_5Br,[6,11] and C_6H_5I[6,12] at 193 nm all indicate that the major channel is fission of the C–X (X=Cl, Br, or I) bond, with both direct and indirect channels being observed. The reason that fission of the C–X bond occurs readily is partly that the energy of the C–X bond is smaller than that of the C–H bond on the phenyl ring, and partly that the dissociation is due to intersystem crossing from a bound (π,π^*) singlet state to a repulsive (n,σ^*) triplet state.[13]

The photodissociation of fluorobenzene (C_6H_5F) is distinct from that of C_6H_5X (X=Cl, Br, or I). The energy of the C–F bond is greater than that of C–H on the phenyl ring, as indicated in the following possible dissociation channels of C_6H_5F:

$$C_6H_5F + h\nu \rightarrow C_6H_5 + F, \quad \Delta H^0 = 534 \text{ kJ mol}^{-1}, \qquad (1)$$

$$C_6H_5F + h\nu \rightarrow C_6H_4F + H, \quad \Delta H^0 \cong 467 \text{ kJ mol}^{-1}, \qquad (2)$$

$$C_6H_5F + h\nu \rightarrow C_6H_4 + HF, \quad \Delta H^0 = 283 \text{ kJ mol}^{-1}, \qquad (3)$$

in which experimental enthalpies of reaction are derived from enthalpies of formation (in kJ mol^{-1}) as follows: C_6H_5F, -115.9 ± 1.3;[14] C_6H_5, 339 ± 8;[15] C_6H_4 (*o*-benzyne), 440 ± 10;[16,17] F, 79.39; H, 218.0; and HF, -273.3 ± 0.7.[18] An experimental enthalpy of formation of C_6H_4F is unknown; a value $\sim$352 kJ mol^{-1} is estimated based on theoretical calculations.[19]

Although the F-elimination channel is energetically accessible, Huang *et al.*[19] observed no evidence of this channel upon photolysis of C_6H_5F at 193 nm (619 kJ mol^{-1}). They employed the multimass ion-imaging technique to find that HF elimination [reaction (3)] is the major channel, whereas H elimination [reaction (2)] is a minor channel; intensities of fragment ions C_6H_4 and C_6H_4F have a ratio $\sim$25:1. Huang *et al.* determined also the distribution of released translational energy for reaction (3) and reported a maximum at 155 kJ mol^{-1} with a decreasing population extending to the

[a)]Authors to whom correspondence should be addressed.
[b)]Electronic mail: shlee@nsrrc.org.tw
[c)]Electronic mail: yplee@mail.nctu.edu.tw

maximum available energy ~336 kJ mol^{-1}.[19] An average translational energy ~159 kJ mol^{-1} was derived from their distribution plot. This value, implying a fraction of $f_t \cong 0.47$ of energy partitioned into translation, is atypically large in view of an exit barrier of only ~60 kJ mol^{-1} predicted with quantum-chemical calculations using CCSD/6-311+G*‖B3LYP/6-31+G*.[19]

Following photodissociation of C_6H_5F at 193 nm, we detected rotationally resolved emission spectra of HF ($1 \leqslant v \leqslant 4$) in the spectral region of 2800–4000 cm^{-1} with a step-scan Fourier-transform spectrometer;[20] an average rotational energy of 15±3 kJ mol^{-1} and an average vibrational energy of $33 \pm {}^{9}_{3}$ kJ mol^{-1} were reported.

We report here our investigation of the branching ratios and distributions of translational energy of fragments on photolysis of C_6H_5F at 193 and 157 nm using fragmentation-translational spectroscopy with a tunable vacuum ultraviolet (VUV) beam from a synchrotron for ionization.

II. EXPERIMENTS

The experimental apparatus is described elsewhere.[21,22] Briefly, the molecular-beam machine coupled with laser photolysis and ionization with synchrotron radiation was employed to investigate the photodissociation of C_6H_5F at 157 and 193 nm. The molecular-beam machine comprises two rotating source chambers, a reaction chamber, and a detection chamber. The molecular beam is rotatable from −20° to 110° with respect to the detection axis. In these experiments we employed only one source chamber, equipped with a pulsed valve (General Valve, series 9, orifice of 0.5 mm) and a skimmer (orifice of 2 mm). A sample cell filled with C_6H_5F was maintained at 283 K to yield a vapor at a pressure of 36 Torr. Ar was bubbled through C_6H_5F liquid to produce a mixture at a pressure of 300 Torr for expansion.

Radiations at 193 and 157 nm, generated from ArF and F_2 excimer lasers, respectively, were focused into the reaction chamber and intersected the molecular beam for photolysis. The photolysis beam was aligned perpendicular to the rotation plane and had a beam size of $\sim 2 \times 7$ mm^2 (WH) for 157 nm and $\sim 2.2 \times 8$ mm^2 for 193 nm at the photolysis region.

Upon photodissociation, fragments were recoiled into a solid angle of 4π sr. Only fragments in a small solid angle entered the ionization region after a free flight along a path of length of 100.5 mm. An undulator served to generate VUV radiation that was directed into the ionization region of the molecular-beam machine via an evacuated path. In addition to the desired fundamental photons, undulator radiation also emits photons at higher harmonics; to absorb these, a windowless gas cell filled with noble gas at a pressure of 10 Torr was employed; Ne, Ar, or Kr was selected depending on the desired photon energy. An additional optical filter of MgF_2 absorbs high harmonic photons effectively when the desired photon energy is less than 10 eV.

After photoionization, a quadrupole mass filter selected product ions at a ratio (m/z) of mass to charge for penetration. A detector (Daly type) counted ions and a multichannel scaler combined with a computer displayed the ion signal with the flight duration. After subtraction of the background signal, detected without laser light, a time-of-flight (TOF) spectrum of a specific fragment is obtained.

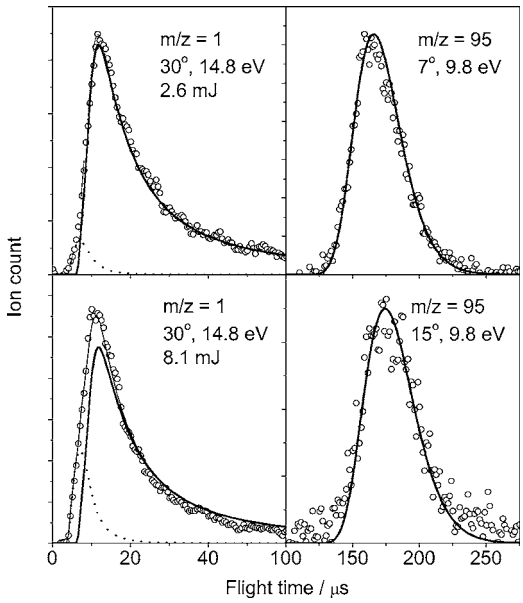

FIG. 1. TOF spectra of H ($m/z=1$) and C_6H_4F ($m/z=95$) produced upon photolysis of C_6H_5F at 157 nm. Laboratory scattering angle, ionizing photon energy (in eV), and laser energy (in microjoules) are shown in each panel. Only the slow component (solid line) of atomic H correlates with C_6H_4F; the rapid component (dotted line) is attributed to two-photon processes. Solid lines are simulation curves using $P(E_t)$ (solid line) in Fig. 5. The thin solid line for plots of $m/z=1$ represents a sum of solid and dotted lines.

III. RESULTS AND ANALYSIS

A. Photolysis of C_6H_5F at 157 nm

Upon photolysis of C_6H_5F at 157 nm, ions H^+, F^+, HF^+, $C_2H_2^+$, $C_6H_4^+$, and $C_6H_4F^+$ were detected at $m/z=1$, 19, 20, 26, 76, and 95 using direct VUV photoionization. To reveal the contribution of multiphoton processes in generation of these products, we measured the dependence of ion signals of these products on the energy of the photolysis laser. The logarithmic plots of signal intensity versus laser energy were fitted to a linear function; plots for H, HF, C_6H_4, and C_6H_4F have slopes of 1.12, 0.96, 0.77, and 0.67, respectively, indicating that reactions (2) and (3) occur with a nearly linear dependence on laser energy; formation of H might also involve some two-photon processes, to be discussed later. In contrast, those for F and C_2H_2 have slopes of 1.67 and 1.62, respectively; they are likely produced via two-photon processes.

With a simulation program *PHOTRAN*, we fitted the TOF spectrum of a product with a trial function of $P(E_t)$ based on forward convolution. Both TOF spectra of two momentum-matched products were fitted with the same $P(E_t)$. The best fits to our experimental data are shown in Figs. 1–4. Figure 1 shows TOF spectra of products H and C_6H_4F. The TOF spectrum of atomic H was deconvoluted into rapid and slow components, shown as dotted and solid lines, respectively; only the slow component correlates with the TOF spectrum of C_6H_4F. The rapid component has a

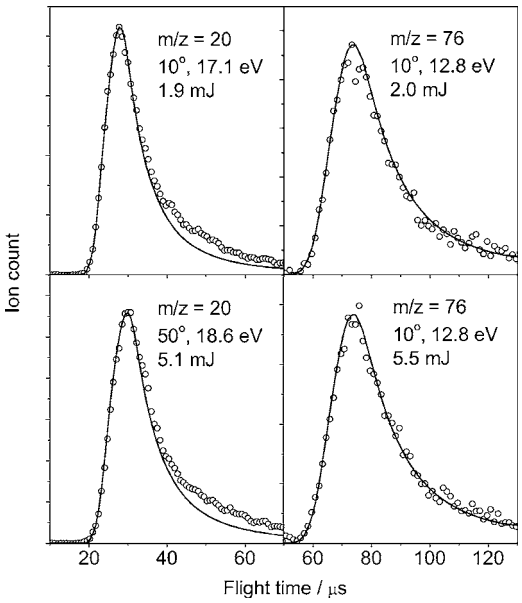

FIG. 2. TOF spectra of HF (m/z=20) and C_6H_4 (m/z=76) produced upon photolysis of C_6H_5F at 157 nm. Laboratory scattering angle, ionizing photon energy (in eV), and laser energy (in microjoules) are shown in each panel. Solid lines are simulation curves using $P(E_t)$ (solid line) in Fig. 6.

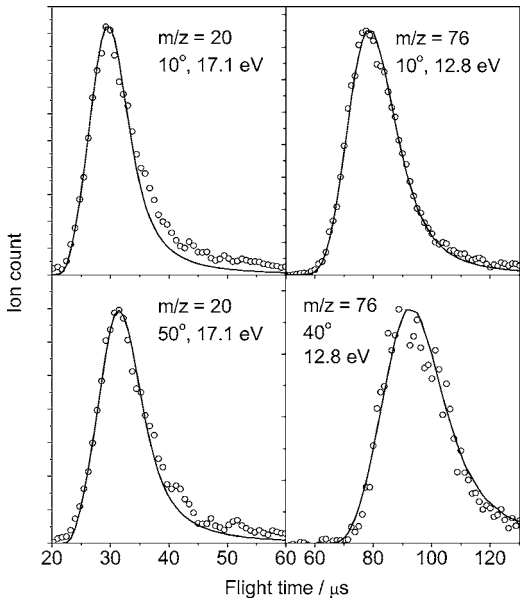

FIG. 4. TOF spectra of HF (m/z=20) and C_6H_4 (m/z=76) produced upon photolysis of C_6H_5F at 193 nm. Laboratory scattering angle and ionizing photon energy (in eV) are shown in each panel. Solid lines are simulation curves using $P(E_t)$ (dotted line) in Fig. 6.

nonlinear dependence on laser energy and is thus attributed to two-photon dissociation, whereas the slow component is associated with the one-photon process. Figure 2 shows TOF spectra of HF and C_6H_4. Although TOF spectra of HF and C_6H_4 correlate satisfactorily with the derived single-component distribution of kinetic energy, $P(E_t)$, a small fraction of the slow component of the TOF spectrum of HF is unaccounted for. Both the major component and this slow component of HF depend linearly on laser energy.

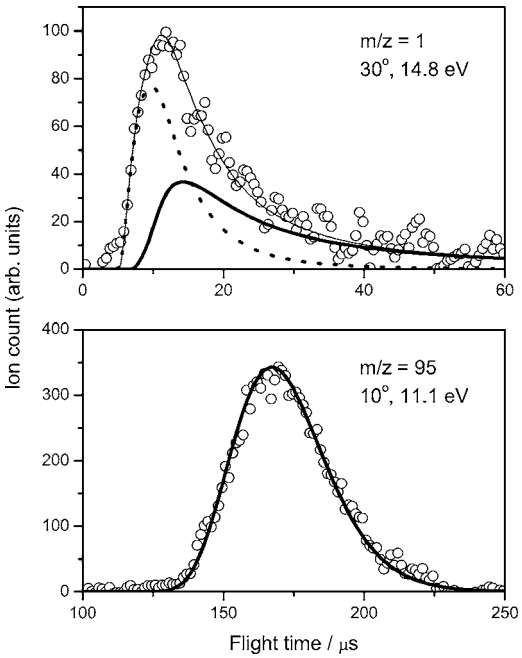

FIG. 3. TOF spectra of H (m/z=1) and C_6H_4F (m/z=95) produced upon photolysis of C_6H_5F at 193 nm. Laboratory scattering angle and ionizing photon energy (in eV) are shown in each panel. Only the slow component (solid line) of atomic H correlates with C_6H_4F; the rapid component (dotted line) is attributed to two-photon processes. Solid lines are simulation curves using $P(E_t)$ (dotted-line) in Fig. 5. The thin solid line for plots of m/z=1 represents a sum of solid and dotted lines.

The dependence of signals of F and C_2H_2 on laser energy indicates that two-photon processes occurred. Their nominal counterparts C_6H_5 and C_4H_3F were unobserved in our experiments.

Minor species arising from fragmentation of photofragments following ionization were observed; their signals depend on the photoionization energy. After subtraction of the duration of ion flight from the total flight duration, daughter ions at m/z=94 ($C_6H_3F^+$), 76 ($C_6H_4^+$), 75 ($C_6H_3^+$), 68 (C_4HF^+), and 50 ($C_4H_2^+$) show TOF distributions the same as that for C_6H_4F. Daughter ions $C_2H_3^+$ and $C_2H_2F^+$ from dissociative ionization of C_6H_4F are minor when ionized at 12.8 eV.

B. Photolysis of C_6H_5F at 193 nm

Photoproducts H, C_6H_4F, HF, and C_6H_4, corresponding to dissociation channels $H+C_6H_4F$ and $HF+C_6H_4$, were observed; their relative intensities and distributions of kinetic energy differed from those observed upon photolysis at 157 nm. Because only a few H atoms were produced at 193 nm, we accumulated its TOF spectrum for 8×10^5 laser shots to improve the ratio of signal to noise. The upper panel of Fig. 3 shows that the TOF spectrum of atomic H comprises two components: a rapid one denoted with a dotted line and a slow one denoted with a solid line. The rapid component is attributed to H atoms produced via a two-photon process as in the case of 157 nm, whereas the slow component is associated with one-photon dissociation [reaction (2)]. Because of a small yield of the C_6H_4F product and of a substantial contribution of the signal from dissociative ionization of C_6H_5F to $C_6H_4F^+$, the C_6H_4F product from reaction (2) was difficult to detect at a small scattering angle. Nevertheless, the lower panel of Fig. 3 shows the TOF spec-

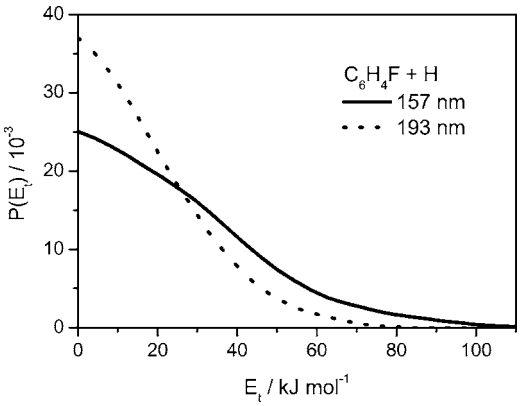

FIG. 5. Distributions of kinetic energy $P(E_t)$ of the channel $C_6H_5F \rightarrow C_6H_4F+H$ at 157 nm (solid line) and 193 nm (dotted line); simulated TOF distributions are shown as solid lines in Figs. 1 and 3 respectively.

trum of C_6H_4F recorded at a scattering angle of 10°. The TOF spectrum of C_6H_4F correlates well with the slow component of the spectrum of atomic hydrogen, shown as the solid line in the upper panel of Fig. 3. After subtraction of the duration of ion flight from the total flight duration, daughter ions of C_6H_4F at $m/z=94$ ($C_6H_3F^+$), 76 ($C_6H_4^+$), 75 ($C_6H_3^+$), 68 (C_4HF^+), and 50 ($C_4H_2^+$) show TOF distributions the same as that for C_6H_4F.

Figure 4 shows TOF spectra of HF and C_6H_4 observed upon photolysis of C_6H_5F at 193 nm. Similar to the case of photolysis at 157 nm, a small fraction of the slow component of HF is unaccounted for with the $P(E_t)$ derived from the TOF spectrum of C_6H_4.

Figures 5 and 6 compare distributions of kinetic energy $P(E_t)$ for reactions (2) and (3), respectively, upon photolysis at 157 nm (solid lines) and 193 nm (dotted lines). The available energy E_{ava}, the average kinetic energy $\langle E_t \rangle = \int P(E_t) E_t dE_t$, and the fraction of translational energy release $f_t = \langle E_t \rangle / E_{ava}$ for product channels C_6H_4F+H and C_6H_4+HF are summarized in Table I. The branching ratios of these two channels are also listed for comparison. The determination of these branching ratios is discussed in the next section.

We measured also the angular anisotropy parameters of products upon photolysis at 157 and 193 nm, and found that,

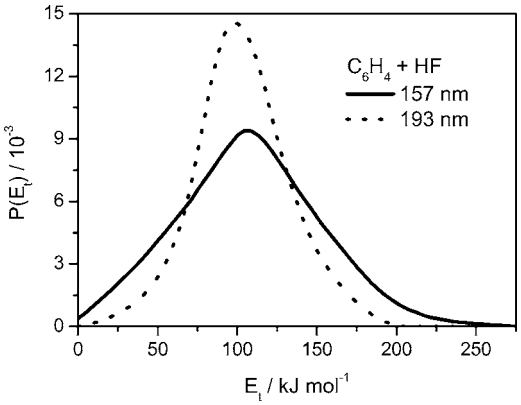

FIG. 6. Distributions of kinetic energy $P(E_t)$ of the channel $C_6H_5F \rightarrow C_6H_4+HF$ at 157 nm (solid line) and 193 nm (dotted line); simulated TOF distributions are shown as solid lines in Figs. 2 and 4 respectively.

TABLE I. Available energies, averaged kinetic energies, fractions of translational energy release, and branching ratios for two channels of dissociation of C_6H_5F upon photolysis at 157 and 193 nm.

Product channel	E_{ava} (kJ mol^{-1})	$\langle E_t \rangle$ (kJ mol^{-1})	f_t (%)	Branching (%)
Photolysis at 193 nm				
$C_6H_5F \rightarrow C_6H_4F+H$	152	18.6	12.2	6±2
$C_6H_5F \rightarrow C_6H_4+HF$	336	103.2	30.7	94±2
Photolysis at 157 nm				
$C_6H_5F \rightarrow C_6H_4F+H$	292	26.8	9.2	39±5
$C_6H_5F \rightarrow C_6H_4+HF$	476	107.8	22.6	61±5

except for atomic hydrogen at 193 nm, all photofragments have an isotropic spatial distribution with $\beta \approx 0$. The slow component of atomic H has a nearly isotropic angular distribution, whereas the rapid component of atomic H associated with dissociation via two-photon processes has a β value of approximately −0.2.

C. Determination of branching ratios

We determined the branching ratios of the H- and HF-elimination channels of fluorobenzene photolyzed at 157 nm by calibration of the relative detection efficiency of the products based on results of photolysis of vinyl fluoride at 157 nm. Vinyl fluoride undergoes four primary and three secondary dissociations; their branching ratios were carefully determined from partitions of TOF spectra of products C_2H_2, C_2HF, F, and H, and from product ratios H/H_2 and C_2H_2/C_2H_3. To determine the branching ratios of fragmentation of fluorobenzene at 157 nm, we compared the TOF spectra of atomic H and HF, derived with photoionization energies of 14.8 and 18.1 eV, respectively, at scattering angles of 30° and 20° for photolysis of vinyl fluoride and fluorobenzene. We calculated the ratio of signals of atomic H and HF produced from vinyl fluoride and fluorobenzene in the center-of-mass frame, and derived branching ratios of the H- and HF-elimination channels of fluorobenzene to be 0.39 and 0.61 based on the well determined product-branching ratios of vinyl fluoride, 0.38:0.62 for H:HF.

Because the ion signal of H atom is small and a large fraction of H atoms are due to two-photon processes at 193 nm, it is difficult to determine branching ratios from the TOF spectra of atomic H and HF. To investigate the branching ratios for decomposition of fluorobenzene at 193 nm, we compared the TOF spectra of C_6H_4F and C_6H_4 at scattering angle 10° with two photoionization energies, 11.1 and 12.8 eV, upon photolysis of fluorobenzene at both 193 and 157 nm. Using the branching ratio of fluorobenzene determined at 157 nm, we determined the branching ratios of the H- and HF-elimination channels of fluorobenzene at 193 nm to be 0.06 and 0.94 from the ratios of signals of C_6H_4F and C_6H_4 in the center-of-mass frame.

IV. DISCUSSION

A. Dependence of product signals on laser energy

Yokoyama *et al.*[2] reported that the signals of photolysis products from benzene exhibited a complicated dependence on laser energy. Upon photolysis of benzene at 193 nm, C_6H_5 and C_5H_3 were produced via a one-photon process, but showed a strong saturation effect. C_3H_3 was produced via a two-photon process, most likely from secondary photolysis of C_6H_6; its signal intensity also showed saturation at large laser energy. Additional secondary products of photodissociation, such as C_6H_3 (C_2H_2, C_4H_3, and C_6H_4), of the primary photofragments C_6H_4 (C_6H_5), were observed; they showed a power dependence consistent with two-photon processes.

Similar results were observed on photolysis of fluorobenzene at 157 nm. HF and atomic H showed a power dependence of order of approximately 1, indicating that these products were produced via one-photon processes. Production of atomic H has a power dependence slightly greater than 1 because of a small contribution of rapid atomic H produced via a two-photon process. The power dependence of counterfragments C_6H_4 and C_6H_4F showed an order much smaller than 1 because secondary photodissociation of C_6H_4 and C_6H_4F occurred. In contrast, atomic F and C_2H_2 have a power dependence of order of ~1.6; this value is attributed to secondary photolysis of primary photofragments or to a direct two-photon dissociation of fluorobenzene. The former mechanism is preferred because the nominal counterparts C_6H_5 and C_4H_3F were unobserved in the present work.

B. Dissociation channel $C_6H_5F \rightarrow C_6H_4F+H$

The energies of C–H bonds for H atoms *ortho*, *meta*, or *para* to the F atom in C_6H_5F vary slightly. Because we are unable to distinguish the small differences among fission of these C–H bonds under the present experimental conditions, we obtain no information about the branching among dissociation of various C–H bonds.

The distributions of translational energy of this channel, shown in Fig. 5, exhibit maxima at zero kinetic energy and extend to ~80 and 110 kJ mol^{-1} for photodissociation at 193 and 157 nm, respectively; the average kinetic energies are 18.6 and 26.8 kJ mol^{-1}, respectively. Such a distribution is characteristic of dissociation without an exit barrier, typical for fission of a bond on the ground-state electronic surface. According to quantum-chemical calculations, the energy ~467 kJ mol^{-1} for the C–H bond implies maximal available energies ~152 and 292 kJ mol^{-1} for photodissociation at 193 and 157 nm, respectively.[20] The fractions of kinetic energy released are thus 12.2% and 9.2% for dissociations at 193 and 157 nm, respectively, as listed in Table I. Hence the photofragment C_6H_4F is expected to be highly internally excited with average internal energies of 133 and 265 kJ mol^{-1} for dissociation at 193 and 157 nm, respectively. Secondary dissociation of the C_6H_4F product is unobservable in the present work. The dissociation of C_6H_5F into C_6H_4+F+H requires an enthalpy of 853 kJ mol^{-1} that exceeds the excitation energy of 759 kJ mol^{-1} upon photolysis at 157.6 nm. Although the enthalpy of formation of C_6H_3F is unknown, we believe that dissociation into C_6H_3F+2H is also negligible.

Huang *et al.*[19] did not report $P(E_t)$ for this channel because the parent ion severely interfered with their image of $m/z=95$ ($C_6H_4F^+$); the intensity of the signal at $m/z=95$ is much smaller than that of parent ions and their mass resolution is limited. Nevertheless, they reported $P(E_t)$ for the channel

$$C_6D_5F + h\nu \rightarrow C_6D_4F + D \tag{4}$$

to have a shape of distribution similar to our results and an average energy ~18 kJ mol^{-1},[19] consistent with our results.

C. Dissociation channel $C_6H_5F \rightarrow C_6H_4+HF$

Upon photolysis at 193 and 157 nm, a negligibly small fraction of the slow component of HF is unaccounted for, according to simulation of the TOF spectrum of HF from a momentum-matched TOF spectrum of C_6H_4. The further decomposition of a small fraction of internally excited C_6H_4 photofragment might account for the discrepancy. Because the discrepancy is small, we are unable to confirm positively the source of deviation.

The distributions of translational energy of this channel, shown in Fig. 6, exhibit maxima at ~100 and 105 kJ mol^{-1} and extend to ~200 and 275 kJ mol^{-1}, respectively, for photodissociation at 193 and 157 nm; the average kinetic energies are 103.2 and 107.8 kJ mol^{-1}, respectively. Such a distribution is characteristic of a dissociation with an exit barrier, typical for molecular elimination on the ground-state electronic surface. Our results differ from that reported previously with a maximum at ~155 kJ mol^{-1} and an average kinetic energy of 159 kJ mol^{-1} using the multimass imaging technique.[19] Considering the characteristics of both techniques, we expect our results to be more reliable.

With $\Delta H^0=283$ kJ mol^{-1} for this channel, the maximal available energies are 336 and 476 kJ mol^{-1} for photodissociation at 193 and 157 nm, respectively. The fractions of kinetic energy release are thus 30.7% and 22.6% for dissociation at 193 and 157 nm, respectively, as listed in Table I. Previous experiments on photolysis of C_6H_5F at 193 nm with time-resolved Fourier-transform infrared (FTIR) emission yield an average rotational energy of 15 ± 3 kJ mol^{-1} and vibrational energy of $33\pm{}^{9}_{3}$ kJ mol^{-1} for HF.[20] Hence the photofragment C_6H_4 is expected to have an average internal energy ~185 kJ mol^{-1} upon photolysis at 193 nm. This energy is less than that of the C–H bond; hence the fraction of C_6H_4 that undergoes further decomposition is expected to be small.

D. Dissociation mechanism

The first three absorption features of benzene in the regions of 230–260, 185–210, and 170–185 nm are assigned to S_1, S_2, and S_3 states, respectively.[23] Fluorobenzene shows a redshift in wavelength for the S_2 band and a blueshift for the S_3 band, compared with absorption of benzene in solution.[24] Accordingly, C_6H_5F is expected to be excited to the S_2 state at 193 nm and to a Rydberg state at 157 nm;[25]

the former is consistent with vertical excitation energy predicted quantum chemically.[13] The asymptote of C_6H_4F $(X\,^2A')+H(^2S)$ correlates with the singlet electronic ground state and a triplet state of C_6H_5F, whereas the asymptote of C_6H_4 $(X\,^1A_1)+HF(X\,^1\Sigma^+)$ correlates with only the electronic ground state of C_6H_5F. Although the channel C_6H_5 $(X\,^2A_1)$ $+F(^2P)$ is energetically accessible, and the predicted intersystem crossing point for dissociation via a repulsive triplet state has an energy (6.33 eV) smaller than that of the 193 nm photon;[13] it was unobserved even upon irradiation at 157 nm.

The small rate of dissociation is attributed to decomposition from the electronic ground state following internal conversion from the initially photoexcited state to the ground state or mediated with a lower electronic excited state. C_6H_5F thus formed on the electronic ground-state surface decomposes according to two competing channels: elimination of atomic H and of HF. The branching for elimination of atomic H increases from 0.06 to 0.39 when photoexcitation energy increases from 619 mJ (at 193.3 nm) to 759 mJ (at 157.6 nm). That the HF-elimination channel has a greater branching ratio than the H-elimination channel indicates that internal conversion is much more efficient than intersystem crossing in C_6H_5F. Because of this efficient internal conversion, aromatic compounds typically have a small rate of dissociation upon excitation at 193 nm; a reported rate is $1\times10^5\ s^{-1}$ for benzene.[3] As the transition state of the four-center HF-elimination channel lies $\sim$80 kJ mol^{-1} below the asymptote of the H-elimination channel, the HF-elimination channel has a greater branching ratio than the H-elimination channel based on the Rice-Ramsperger-Kassel-Marcus (RRKM) theory. Branching ratios of the two dissociation channels become similar with increasing energy of excitation. The rate of dissociation of C_6H_5F is much smaller than the rotational frequency of C_6H_5F, which accounts for the nearly isotropic angular distributions of products.

There are two possible channels for HF elimination. In our previous work, we performed calculations to characterize transition states for four-center (TS4) elimination and H shift (TS2) followed by three-center (TS3) elimination of C_6H_5F with the B3LYP/6-311G(d,p) density-functional theory.[20] These calculations yield barriers of 497 and 387 kJ mol^{-1} for three-center and four-center elimination channels, respectively; these barriers are within 17 kJ mol^{-1} of those predicted using the CCSD method.[19] The three-center elimination proceeds via a transition state TS2 with a barrier of 389 kJ mol^{-1} to form iso-C_6H_5F with an energy nearly identical to that of TS2, followed by a further barrier of 108 kJ mol^{-1} to reach TS3. According to calculated energies for transition states of three-center and four-center HF-elimination channels, the exit barriers are 166 and 56 kJ mol^{-1}, respectively.[20] The rates of dissociation of C_6H_5F via four-center and three-center elimination channels at energy 619 kJ mol^{-1} were estimated with a microcanonical transition-state theory to be 1.1×10^6 and $2.2\times10^3\ s^{-1}$, respectively, by Huang *et al.*[19] and 8.7×10^5 and 89 s^{-1}, respectively, by Wu *et al.*[20] Accordingly, production of HF via the three-center elimination path on the ground electronic surface is negligible.

Our observation of average kinetic energies of 103.2 and 107.8 kJ mol^{-1} for the photodissociation of C_6H_5F at 193 and 157 nm exceeds substantially the exit barrier 56 kJ mol^{-1} for four-center elimination. One possible reason might be that a large fraction of trajectories pass through regions of high energy instead of regions near the saddle point of TS4. Palmer *et al.*[26] used a Monte Carlo self-consistent-field (MC-SCF) method with a 4-31G basis set to investigate the conical intersections of benzene between S_2 and S_1 and between S_1 and S_0 surfaces. They found that, at the two conical intersections, benzene has a structure in which a carbon atom rises above the original molecular plane; the corresponding C–H bond tends to be perpendicular to the original molecular plane. Analogously, we surmise that fluorobenzene has a structure similar to that of benzene at conical intersections at which the C–F bond might have a preference for puckering. If fluorobenzene retains a large energy in the out-of-plane motion of the C–F group after internal conversion, the elimination of HF would proceed through an effective exit barrier that is much greater than the saddle point of TS4.

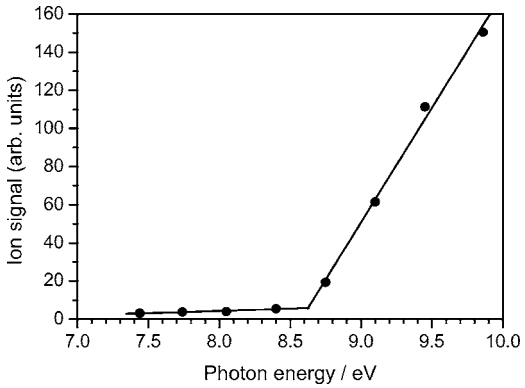

FIG. 7. Photoionization yield of C_6H_4F in the energy range of 7.5–9.8 eV. The C_6H_4F product was created from photolysis of fluorobenzene at 157 nm, and its TOF spectra were detected at a laboratory angle of 7°. C_6H_4F ions in the interval of 100–270 μs of flight duration were integrated. No correction is made for a small variation of photon flux with photon energy. Two fitted lines intersect at $\sim$8.6 eV.

E. Ionization of C_6H_4F

Ionization energies of several aromatic compounds and their fragments due to elimination of a hydrogen atom have been reported. The ionization energy of benzene (C_6H_6) is 9.24384 ± 0.00006 eV,[27] whereas that of the phenyl radical (C_6H_5) was reported to be much smaller, 8.32 ± 0.04 eV.[28] In contrast, the ionization energy of *p*-bromophenyl radical (*p*-C_6H_4Br), 9.04 eV,[29] is 0.04 eV greater than the value 9.00 eV for bromobenzene (C_6H_5Br).[30] The energy of the $F-C_6H_5$ bond is $\sim$69 kJ mol^{-1} greater than that of the $H-C_6H_5$ bond, whereas the energy of the $Br-C_6H_5$ bond is $\sim$129 kJ mol^{-1} less than that of the $H-C_6H_5$ bond.[14] Moreover, C_6H_5F has an ionization energy only 0.04 eV less than that of C_6H_6 whereas that of C_6H_5Br is 0.24 eV less than that of C_6H_6.[30] Considering bond energy and ionization energy, C_6H_5F behaves more similarly to C_6H_6 than to C_6H_5Br.

Figure 7 indicates that the ion signal of C_6H_4F decreases greatly as the photon energy decreases from 10 to 8.6 eV; a small ion signal persists for energies as small as 7.4 eV. The

small ion signal below 8.6 eV is attributed partly to ionization of internally hot C_6H_4F and partly to ionization of C_6H_4F by the residual white light existing as an emission continuum underlying the harmonic photon peaks from the undulator. White light with an energy less than the cutoff ($\sim$10 eV) of a MgF_2 window passes the optical filter and subsequently ionizes C_6H_4F. We determined the ionization energy of C_6H_4F to be 8.6±0.2 eV from the intersection of the two guidelines shown in Fig. 7; this value is nearer the ionization energy of C_6H_5 than that of *p*-C_6H_4Br. Although the C_6H_4F product has an average internal energy of 265 kJ mol^{-1} (2.75 eV) from the energy available upon photolysis at 157 nm, most internal energy is expected to distribute among various vibrational modes and to have only a small effect on the ionization energy.

The dissociations of $C_6H_4F^+$ into $C_6H_3F^+$+H, $C_6H_4^+$+F, and $C_6H_3^+$+HF have smaller enthalpies of reaction than the dissociations into C_6H_3F+H^+, C_6H_4+F^+, and C_6H_3+HF^+, respectively, which reflect the preferential observation of daughter ions $C_6H_3F^+$, $C_6H_4^+$ and $C_6H_3^+$ rather than H^+, F^+, and HF^+. In contrast, consideration of enthalpy fails to account for the finding that the yields of C_4HF^+ and $C_4H_2^+$ are greater than those of $C_2H_3^+$ and $C_2H_2F^+$ upon photoionization of C_6H_4F at 12.8 eV. Because the ionization energy of 8.25 eV of C_2H_3 (Ref. 31) is smaller than that of C_4HF, 10.1 eV,[32] the dissociation of $C_6H_4F^+$ to $C_2H_3^+$+C_4HF has an enthalpy of reaction of 1.85 eV smaller than that for the formation of C_2H_3+C_4HF^+. We suggest that $C_6H_4F^+ \rightarrow C_2H_3^+$+$C_4HF$ might have a larger barrier than $C_6H_4F^+ \rightarrow C_2H_3$+$C_4HF^+$. The former process behaves like a dissociation into two molecular fragments that typically has a large barrier, whereas the latter process behaves like a dissociation to two radicals that typically has no barrier. Analogously, we expect $C_6H_4F^+ \rightarrow C_2H_2F^+$+$C_4H_2$ to have a greater barrier than $C_6H_4F^+ \rightarrow C_2H_2F$+$C_4H_2^+$. C_4H_2 has an ionization energy of 10.17 eV, 0.07 eV greater than C_2HF.[32] An ionization energy of C_2H_2F is unavailable from the literature.

V. CONCLUSION

We employed fragmentation-translational spectroscopy utilizing a tunable source of vacuum ultraviolet radiation from a synchrotron to investigate the photodissociation dynamics of C_6H_5F at 157 and 193 nm. The products H, C_6H_4F, HF, and C_6H_4 correlate to two major dissociation channels: C_6H_4F+H and C_6H_4+HF. The dominant channel, elimination of HF, has a branching ratio $\sim$0.94 and 0.61 and average kinetic energies $\sim$103 and 108 kJ mol^{-1} for photolysis at 193 and 157 nm, respectively; it proceeds on the S_0 ground-state electronic surface following internal conversion from the electronically excited state of C_6H_5F. The channel for fission of the C–H bond has a branching ratio $\sim$0.06 and 0.39 and average release of kinetic energies $\sim$18.6 and 26.8 kJ mol^{-1} for photolysis at 193 and 157 nm, respectively. The small rate of dissociation of C_6H_5F leads to isotropic angular distributions of products. Based on the available energy and the observed release of translational energy and internal energy of HF, the fragment C_6H_4F is expected to be highly internally excited. We determined the ionization energy of C_6H_4F to be 8.6±0.2 eV.

ACKNOWLEDGMENTS

The National Science Council of Taiwan (Grant Nos. NSC95-2119-M-009-032 and NSC94-2113-M-213-004) and the National Synchrotron Radiation Research Center supported this work.

[1] A. M. Mebel, M. C. Lin, D. Chakraborty, J. Park, S. H. Lin, and Y. T. Lee, J. Chem. Phys. **114**, 8421 (2001) and references therein.
[2] A. Yokoyama, X. Zhao, E. J. Hintsa, R. E. Continetti, and Y. T. Lee, J. Chem. Phys. **92**, 4222 (1990).
[3] S.-T. Tsai, C.-K. Lin, Y. T. Lee, and C.-K. Ni, J. Chem. Phys. **113**, 67 (2000).
[4] S.-T. Tsai, C.-L. Huang, Y. T. Lee, and C.-K. Ni, J. Chem. Phys. **115**, 2449 (2001).
[5] C.-K. Lin, C.-L. Huang, J.-C. Jiang, H. H. Chang, Y. T. Lee, S. H. Lin, and C.-K. Ni, J. Am. Chem. Soc. **124**, 4068 (2002).
[6] A. Freeman, S. C. Yang, M. Kawasaki, and R. Bersohn, J. Chem. Phys. **72**, 1028 (1980).
[7] T. Ichimura, Y. Mori, H. Shinohara, and N. Nishi, Chem. Phys. **189**, 117 (1994).
[8] T. Ichimura, Y. Mori, H. Shinohara, and N. Nishi, Chem. Phys. **122**, 51 (1985).
[9] K.-L. Han, G.-Z. He, and N.-Q. Lou, Chem. Phys. Lett. **203**, 509 (1993).
[10] G.-J. Wang, R.-S. Zhu, H. Zhang, K.-L. Han, G.-Z. He, and N.-Q. Lou, Chem. Phys. Lett. **288**, 429 (1998).
[11] H. Zhang, R.-S. Zhu, G.-J. Wang, K.-L. Han, G.-Z. He, and N.-Q. Lou, J. Chem. Phys. **110**, 2922 (1999).
[12] M. Dzvonik, S. Yang, and R. Bersohn, J. Chem. Phys. **61**, 4408 (1974).
[13] Y.-J. Liu, P. Persson, and S. Lunell, J. Phys. Chem. A **108**, 2339 (2004).
[14] *CRC Handbook of Chemistry and Physics*, 78th ed., edited by D. R. Lide (CRC, New York, 1997).
[15] W. Tsang, in *Energetics of Organic Free Radicals*, edited by J. A. Martinho Simoes, A. Greenberg, and J. F. Liebman (Blackie Academic and Professional, London, 1996), pp. 22–58.
[16] J. M. Riveros, S. Ingeman, and N. M. M. Nibbering, J. Am. Chem. Soc. **113**, 1053 (1991).
[17] P. G. Wenthold and R. R. Squires, J. Am. Chem. Soc. **113**, 7414 (1991); **116**, 6401 (1994).
[18] M. W. Chase, Jr., J. Phys. Chem. Ref. Data Monogr. **9**, 1 (1998).
[19] C.-L. Huang, J.-C. Jiang, A. M. Mebel, Y. T. Lee, and C.-K. Ni, J. Am. Chem. Soc. **125**, 9814 (2003).
[20] C.-Y. Wu, Y.-J. Wu, and Y.-P. Lee, J. Chem. Phys. **121**, 8792 (2004).
[21] C.-C. Wang, Y. T. Lee, J. J. Lin, J. Shu, Y.-Y. Lee, and X. Yang, J. Chem. Phys. **117**, 153 (2002).
[22] S.-H. Lee, Y.-Y. Lee, Y. T. Lee, and X. Yang, J. Chem. Phys. **119**, 827 (2003).
[23] A. Hiraya and K. Shobatake, J. Chem. Phys. **94**, 7700 (1991).
[24] J. Petruska, J. Chem. Phys. **34**, 1120 (1961).
[25] K. Bowden and E. A. Braude, J. Chem. Soc. **1952**, 1068.
[26] I. J. Palmer, I. N. Ragazos, F. Bernardi, M. Olivucci, and M. A. Robb, J. Am. Chem. Soc. **115**, 673 (1993).
[27] G. I. Nemeth, H. L. Selzle, and E. W. Schlag, Chem. Phys. Lett. **215**, 151 (1993).
[28] V. Butcher, M. L. Costa, J. M. Dyke, A. R. Ellis, and A. Morris, Chem. Phys. **115**, 261 (1987).
[29] O. Nuyken and K. Messmer, Org. Mass Spectrom. **12**, 106 (1977).
[30] S. Fujisawa, K. Ohno, S. Masuda, and Y. Harada, J. Am. Chem. Soc. **108**, 6505 (1986).
[31] J. A. Blush and P. Chen, J. Phys. Chem. **96**, 4138 (1992).
[32] G. Bieri, A. Schmelzer, L. Asbrink, and M. Jonsson, Chem. Phys. **49**, 213 (1980).